Effect of Superficial Gas Velocity on Bubbling Fluidized Bed Biomass Gasification

[*]Cornelius Emeka Agu, Britt M.E. Moldestad

Department of Process, Energy and Environmental Technology, University College of Southeast Norway, 3918 Porsgrunn, Norway

*cornelius.e.agu@usn.no; britt.moldestad@usn.no

Tel: +4740987735

Abstract

This study investigates the behaviour of bubbling fluidized beds during biomass gasification using the variation of superficial gas velocity at different temperatures and air flowrates. The operating window is defined as the gas velocity between the minimum fluidization and slugging velocities, which are computed using the correlations in the literature. The analysis shows that the operating gas velocity depends on the amount of char accumulated in the bed. An increase in the char accumulation results in higher minimum fluidization and slugging velocities of the bed mixture. Based on this, the gas velocity ratio to achieve the desired operating regime of a fluidized bed is higher when the biomass accumulation is considered.

Keywords: Biomass; Gasifier; Air-fuel ratio; CPFD; Bubbling fluidized bed

1 Introduction

Fluidized beds have numerous advantages in chemical processes, for example, biomass gasification. Such benefits include the excellent gas-solid mixing that can lead to uniform heat and mass distribution within the reactor. In a bubbling fluidized bed, the solids materials are retained within the dense phase, ensuring high solid inventory and a stable pressure drop. However, a drawback of this technology is the limitation to gas flow rate imposed by the hydrodynamics of the bed material [1]. For a given material, the bed is in the bubbling regime when the gas velocity is not too high above the minimum fluidization velocity at the operating condition. When the gas velocity is very high, the bed may transit into slugging, turbulent flow or fast fluidization [1]. The flow of slugs in a bed may result in gas bypass and high fluctuation of the bed. Within the bubbling regime, the operating velocity usually lies between the minimum fluidization and slugging velocity.

An increase in the gas yield during the solid fuel conversion enhances the gas velocity at the operating temperature. With changes in the temperature and pressure, the fluid properties as well as the particle-particle interactions vary, leading to changes in the flow behaviour in the fluidized bed reactor. In extreme cases, this may lead to changes in the fluidization type [2]. The common observations to these changes is the effect of temperature on the transition of fluidized bed regimes as have been demonstrated in different studies. Increasing the bed temperature decreases the minimum fluidization velocity of Geldart A and B particles and increases those of Geldart D particles [3, 4] due to changes in the fluid properties. Moreover, the gas velocities at the onset of slugging and turbulent fluidization increase with increasing temperature due to changes in the fluid properties and a decrease in the bubble size, thereby leading to a smooth fluidization of the bed [5, 6].

In designing bubbling fluidized bed reactors, selecting the suitable gas velocities for stable operations while achieving the desired gas yields and composition is a critical issue. This study is aimed at investigating the effect of gas velocity in a bubbling fluidized bed during the biomass gasification. The study is based on the theoretical equations developed for fluidized bed behaviour. The semi-empirical models are applied to simulate the minimum fluidization and slugging velocities with and without accumulation of biomass in the bed for a given reactor size and operating condition. In addition, the possibility of solids entrainment at the operating temperature and different gas velocities is simulated using the computational particle-fluid dynamics (CPFD) code.

2 Theory: Correlations for minimum fluidization and slugging velocities

Fluidized bed reactors usually contains a mixture of different types of particles. Each particle type influences the behaviour of the bed. The bubble properties (size and rise velocities) and transition velocities from one regime to another differ significantly from those of pure solid particles. The extent to which the bed behaviour is affected by each solid component depends on the amount of the individual solids in the bed. In biomass gasification reactors, the solid particles include the raw biomass, bed material, ash and char particles. For simplicity, the ash content of the fuel can be neglected since it is relatively low compared to other particles in the bed. Raw biomass and char particles can be lumped into one solid component using their average mass density and particle size. The resulting bed is a binary mixture consisting of the lumped biomass and bed material particles.

The minimum fluidization velocity of a binary mixture of biomass and bed material can be obtained from different correlations [7, 8] for a given amount of biomass particles. In general, the minimum fluidization velocity of a bed can be computed by balancing the bed weight per unit area with the Ergun [9] equation as expressed below.

$$\frac{1.75}{\varepsilon_{mf}^3}\left(\frac{\rho_f U_{mf} d_s}{\mu_g}\right)^2 + \frac{150(1-\varepsilon_{mf})}{\varepsilon_{mf}^3}\left(\frac{\rho_g U_{mf} d_s}{\mu_g}\right) = Ar \tag{1}$$

$$Ar = \frac{d_s^3 \rho_g (\rho_s - \rho_g) g}{\mu_g^2} \tag{2}$$

where, U_{mf} and ε_{mf} are the superficial gas velocity and bed void fraction at the minimum fluidization condition, respectively. Ar is the Archimedes number, ρ_g is the fluid density, $\mu_g$is the fluid dynamic viscosity, ρ_s is the density and d_s is the average diameter of the particles. For a bed of sand-like particles, Eq. (1) can be reduced as given in Eq. (3) [10].

$$U_{mf} = \frac{\mu_g}{\rho_g d_s}\left[-33.67 + \sqrt{((33.67)^2 + 0.0408Ar)}\right] \tag{3}$$

Equation (1) can also be used to predict the U_{mf} of a binary mixture of biomass and bed material as described in Agu et al. [11], where the particle diameter and density are replaced with the respective average values d_{sm} and ρ_{sm} for the mixture. The mixture void fraction ε_{mfm} is computed from [11]

$$\varepsilon_{mfm} = 1 - \frac{1-\varepsilon_{mfp}}{\left[\left((1-\varepsilon_{mfp}) - \varepsilon_{mfb}\left(1 - \left(\frac{d_{sp}}{d_{sb}}\right)^{\beta x_p}\right)\left(\frac{d_{sp}}{d_{sb}}\right)\right)\frac{y_b}{(1-\varepsilon_{mfb})} + y_p\right]} \tag{4}$$

$$\beta = 0.623\left(\frac{d_{sp}\rho_{sp}}{d_{sb}\rho_{sb}}\right)^{-0.61} \tag{5}$$

Here, ε_{mfp} and ε_{mfb} are the individual void fractions of the bed material and biomass particles at minimum fluidization, respectively, and d_{sp}, d_{sb}, ρ_{sp} and ρ_{sb} are the corresponding particle diameter and density. y_p and y_b are the volume fraction of the different components in the mixture, where x_p is the mass fraction of the bed material.

The minimum slugging velocity U_{msm} of the binary mixture increases significantly with an increase in the amount of biomass in the bed [12]. For biomass volume fraction less than 40%, the ratio, U_{msm}/U_{msp} is independent of biomass properties, where U_{msp} is the minimum slugging velocity of the bed material. Correlating the results obtained in different beds of sand-wood chip and sand-wood pellet mixtures, U_{msm}/U_{msp} can be predicted from [12]

$$\frac{U_{msm}}{U_{msp}} = e^{1.13 y_b} \tag{6}$$

Among other models [13, 14], the value of U_{msp} can be predicted from the following equation as given in Agu et al. [15].

$$\frac{U_{msp}}{U_{mfp}} = 1 + 2.33U_{mfp}^{-0.027}\left(\varphi^{0.35}c_t^{a_t} - 1\right)\left(\frac{h_0}{D}\right)^{-0.588} \quad (7)$$

Here, φ is the particle sphericity, h_0 is the initial bed height and D is the bed diameter. The values of the parameters a_t and c_t are as described in [15] depending on the Archimedes number, where $Ar > 400$.

The amount of biomass in a bed depends on the biomass residence time at the operating condition for a given air-fuel ratio (AFr). For a steady biomass mass flowrate $\dot{m}_b$, the mass fraction of biomass x_b accumulated in a bed of mass m_p can be estimated from the following equations proposed by Agu et al. [16].

$$\frac{x_b}{1-x_b} = (1-\alpha)\gamma_{char}(t_e - t_d)\frac{\dot{m}_b}{m_p} \quad (8)$$

$$t_d = 681X_b^{0.028}\left(\frac{U_0}{U_{mfp}}\right)^{-0.3} \quad (9)$$

$$t_e = 4055X_b^{0.278}\left(\frac{U_0}{U_{mfp}}\right)^{-0.185} \quad (10)$$

$$\gamma_{char} = 0.414X_b^{0.245}\left(\frac{U_0}{U_{mfp}}\right)^{-0.463} \quad (11)$$

$$X_b = \left[4055\frac{\dot{m}_b}{m_p}\left(\frac{U_0}{U_{mfp}}\right)^{-0.185}\right]^{1.385} \quad (12)$$

where $0.45 < \alpha < 0.7$ is the fraction of time over the char residence time $(t_e - t_d)$ that measures the extent of char conversion during one cycle of an ideal plug flow process. γ_{char} is the amount of char released at the completion of biomass devolatilization (pyrolysis) and X_b is the ratio of the mass of biomass loaded over the period t_e to the mass of the bed material.

3 Computational Model

To investigate the effect of gas velocity on vertical movement of particles in hot reactors, the fluidized bed behaviour was simulated using Barracuda VR software. Barracuda is the commercially developed platform for implementing computational particle-fluid dynamics (CPFD) scheme. CPFD is based on the multiphase-particle-in-cell (MP-PIC) concept introduced by Andrew and O'Rourke [17]. In the CPFD scheme, the Euler-Lagrangian modelling approach is applied for fluid volume and particle tracking in gas-solid systems. With the MP-PIC concept, a computational particle represents a large number of particles, which have similar properties. The grouping of particles in CPFD code makes the simulation faster, thereby increasing its application to industrial systems. Detailed descriptions of the CPFD model and its numerical scheme can be found in Chen et al. [18].

4 Material and bed properties

In this study, sand particles are considered as the bed material and wood chips as the biomass. Table 1 gives the properties of these particles at the ambient conditions.

In the temperature range 25 – 550 ºC, the minimum fluidization velocity of the sand particles were measured using the curves of pressure drop versus superficial air velocity at different temperatures. The experiments were conducted in a cylindrical column of diameter 0.1 m and height 1.0 m. The minimum fluidization velocity for the 610 µm sand particles at the different temperatures were correlated as given by Eq. (13), where $T_0 = 25$ ˚C, $\rho_{g0} = 1.18$ kg/m^3 and $U_{mf0} = 0.232$ m/s.

Table 1. Bed material and biomass at ambient conditions.

Materials	$\boldsymbol{\rho_p}$ (kg/m^3)	$\boldsymbol{d_s}$ (mm)	$\boldsymbol{\varphi_s}$ (-)	$\boldsymbol{\varepsilon_{mf}}$ (-)	$\boldsymbol{U_{mf}}$ (m/s)
Wood chips	423	6.87	0.75	0.57	1.27
Sand	2650	0.293	0.86	0.46	0.232

$$U_{mf} = \frac{\rho_{g0}}{\rho_g} U_{mf0}\{0.19 + 0.787 \exp[-0.0045(T - T_0)]\} \quad (13)$$

Fig. 1 compares the minimum fluidization velocities computed using Eq. (13) with those obtained from Eq. (1) as well as the CPFD simulations at different temperatures. All the results show a decrease in the minimum fluidization velocity with increasing temperature. Both the CPFD simulation and the Wen and Yu correlation agree to some extent with Eq. (13) within a certain temperature range. The results from Eq. (1) are better than those from the simulations for temperatures above 200 ˚C. The simulation result at the ambient temperature perfectly matches the experimental value, but the deviation at higher temperature increases as the temperature increases. As both the correlation, Eq. (1) and the CPFD simulations give results with a trend similar to the experimental data and with good numerical accuracies, both models are used for prediction of the bed behaviour in the further analyses.

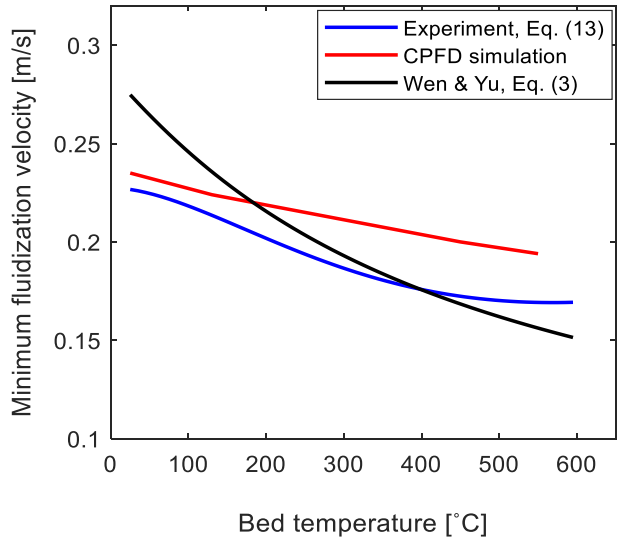

Fig. 1. Variation of minimum fluidization velocity with temperature, comparing experimental data with the CPFD simulation results and the Wen & Yu correlation; particle size: 610 µm.

5 Results and discussion

For particle size as large as 600 µm, the inlet superficial gas velocity used in most studies on bubbling fluidized bed gasification, is usually within 2 – 3 times the minimum fluidization velocity of the bed material. When biomass is introduced in the reactor, the increase in the gas mass flowrate increases the gas velocity through the bed at the operating conditions. Assuming a full conversion, the total mass flowrate of gas at steady state can be obtained as $(\dot{m}_{air} + \dot{m}_{bio})$, neglecting the ash content of the fuel. Here, $\dot{m}_{air}$ and $\dot{m}_{bio}$ are the mass flowrates of air and biomass, respectively. Considering gasification of wood chips at an equivalence ratio of 0.25, a value of 1.5 can be obtained for air to biomass mass flowrate ratio. Based on this ratio, and neglecting the difference between the air density and the total gas density, the superficial gas velocity in the bed at full conversion can be approximated to $1.66U_0$, where U_0 is the superficial air velocity at the operating condition. The effect of this total gas velocity depends on how evenly the bed solid species are mixed since biomass particle segregation can occur within the bed despite the fuel feeding position. Assuming a perfect mixing of the solid particles, the gas velocity can be considered uniform over the entire bed volume.

5.1 Neglecting the biomass accumulation

Fig. 2(a) shows the influence of temperature on the bed behaviour of the 610 μm sand particles at two different constant air mass flowrates, $\dot{m}_{air} = 2(\rho U_{mf})_{opt} A_0$ and $\dot{m}_{air} = 3(\rho U_{mf})_{opt} A_0$, which are assumed to represent cases without any reaction. Fig 2(b) shows the behaviour for the corresponding cases at full conversion. Here, the values of $(\rho U_{mf})_{opt}$ are obtained at the reactor operating temperature 900 ˚C, in which $U_{mf} = 0.187$ m/s based on the correlation given by Eq. (13). The plotted data are the superficial gas velocities U_0 and the transition velocities U_{mf} and U_{ms} at different temperatures. The minimum slugging velocity was computed from Eq. (7) at the bed aspect ratio, $h_0/D = 2.5$ and the superficial air velocity was obtained from $U_0 = \dot{m}_{air}/\rho A$, where the air density ρ is at the different temperatures. Due to decreasing gas density, the operating gas velocity U_0 increases with an increase in temperature at a constant mass flowrate. The gas velocity U_{ms} at the onset of slugging also increases as the temperature is increased. From figures, the bed is fluidized (i.e. $U_0 > U_{mf}$) within the temperature range for the respective mass flowrates.

With an increase in temperature, the bed remains in the bubbling regime until the operating velocity line crosses the minimum slugging velocity line. This never occurs in Fig. 2(a) even at the higher mass flowrate. This shows that if the bed is maintained at a gas velocity of $3U_{mf}$ at the operating conditions, the bed will remain in the bubbling regime. However, with a full conversion, the behaviour is completely different as shown in Fig. 2(b); the bed slugs at both total mass flowrates.

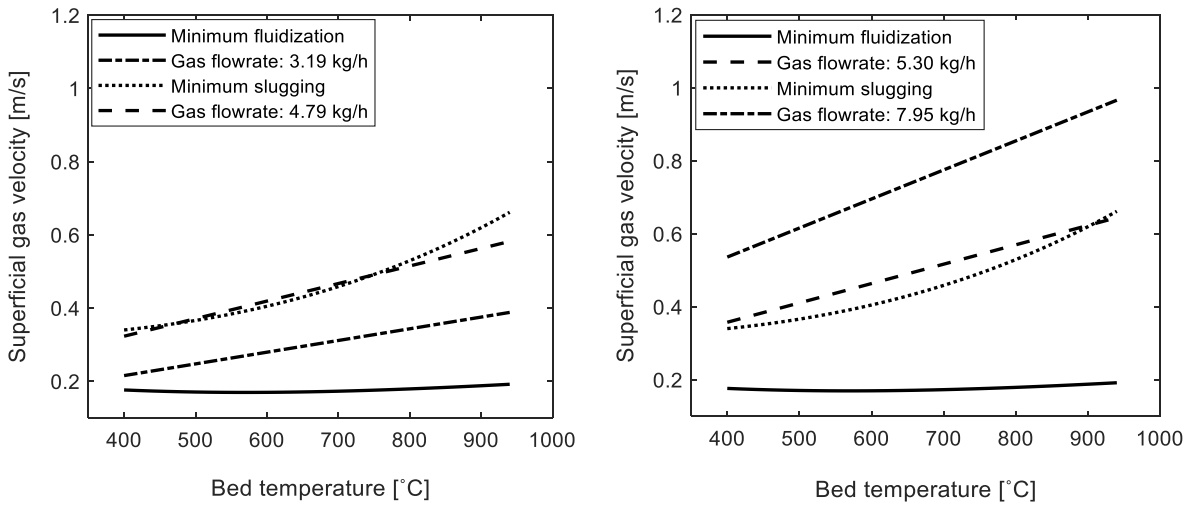

(a) (b)

Fig. 2. Behaviour of bed of sand particles, 610 μm at different temperature and constant mass flowrates, $\dot{m}_{air}$ (a) $(2\rho U_{mf})_{opt} A_0 = 3.19$ and $(3\rho U_{mf})_{opt} A_0 = 4.79$ kg/h (b) $1.66 \cdot (2\rho U_{mf})_{opt} A_0 = 5.30$ and $1.66 \cdot (3\rho U_{mf})_{opt} A_0 = 7.95$ kg/h.

In a bed of larger particles, bubbles can easily grow into slugs. Aside reduction in the gas residence time at higher gas velocities, there are also possibilities of particle attrition and entrainment of fines especially when the reaction column is not tall enough. If a complete reaction is assumed at the operating temperature, the increase in the total gas flowrate may also increase these effects. The effect of gas velocity on the distribution of solids along the bed axis is shown in Fig. 3 for the 610 μm sand particles. The gas flowrates are the same as those used in Fig. 2. In the CPFD simulations, the initial bed height was 25 cm and the initial solids fraction was 0.545. The contours of solids fraction (captured after 20 s) show that as gas velocity increases, the possibility of particles being dragged into the freeboard increases. The time-averaged solids fractions at different positions are shown in Fig. 3(e). In these results, the flow regime of the bed at different gas velocities can be identified as described in Kunii and Levenspiel [1]. The result shows that at the gas velocities $U_0 = 2U_{mf}$ and $U_0 = 3U_{mf}$, the bed is in the bubbling regime, but in the slugging/turbulent flow regime at the two larger gas velocities. In addition, Fig. 3(e) clearly shows that the amount of solids in the freeboard increases as the gas flowrate is

increased, and the particles reach higher up in the column when a higher velocity is used. There are traces of solids in the column up to a height of 70 cm. At this position, the respective solids fractions are $4{\cdot}10^{-7}$, $6{\cdot}10^{-6}$, $6{\cdot}10^{-6}$ and $5{\cdot}10^{-5}$. Especially for the velocity $U_0 = 4.98U_{mf}$, this shows that there is a possibility of particle entrainment from the column.

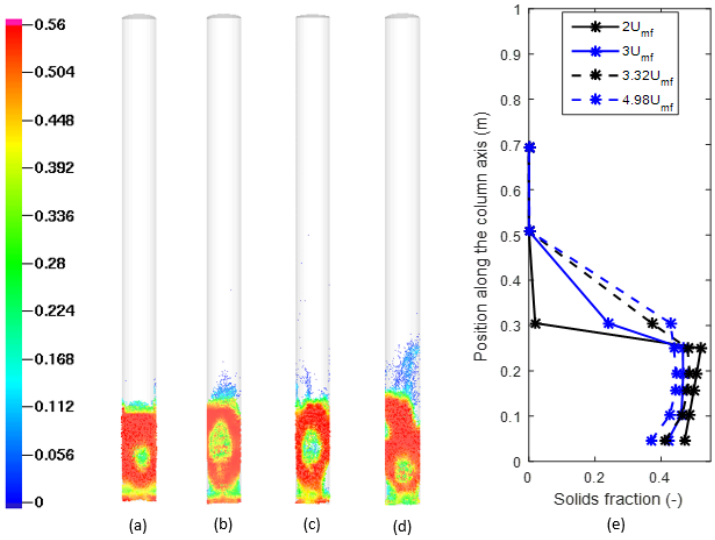

Fig. 3. Bed behaviour simulated using CPFD Barracuda for 610 µm sand particles at 900 ˚C showing the solids fraction distributions captured after 20 at different superficial air velocities (a) $U_0 = 2U_{mf}$ (b) $U_0 = 3U_{mf}$ (c) $U_0 = 3.32U_{mf}$ (d) $U_0 = 4.98U_{mf}$ and (e) the time-average axial distribution of solids fraction.

5.2 Considering the biomass accumulation

By considering the biomass accumulation, Eq. (8) was used to estimate the amount of unconverted char in the bed at the given operating conditions. Fig. 4(a) shows the values of x_b at different air-fuel ratios and constant biomass flowrate 2 kg/h. The result is based on a 10 cm diameter bed containing the 610 µm sand particles at initial height of 25 cm. As shown in the figure, x_b decreases with increasing AFr due to increasing amount of the fuel particles converted. The bed behaviour at the different AFr values is shown in Fig. 4(b). While the values of U_{mf} and U_{ms} of the bed mixture decrease, the gas velocity through the bed increases with increasing air-fuel ratio. For AFr < 1.4, the incoming air velocity is too low to maintain the fluidization of the bed as the accumulation is relatively high. However, with an increase in the total gas flow at the completion of biomass pyrolysis, the bed is fluidized even at AFr value of 1.0. It should be noted that at a low air velocity, the conversion will be delayed, thus the full conversion gas velocity will be rarely achieved at air-fuel ratio < 6. If the total gas yield at full conversion acts on the bed evenly, the bed will remain in the bubbling regime up to AFr = 2.3. The shaded portion in Fig. 4(b) should therefore represents the safe operating window for the system. At the 2.3 air-fuel ratio, the incoming air velocity, $U_0/U_{mfp} = 3$. On the contrary, when the biomass accumulation is not considered, the maximum air velocity within the bubbling window at 900 ºC is $U_0/U_{mfp} = 2$ as can be seen in Fig 2. This indicates that the amount of unconverted biomass must be considered when selecting the gas velocity for a fluidized bed operation.

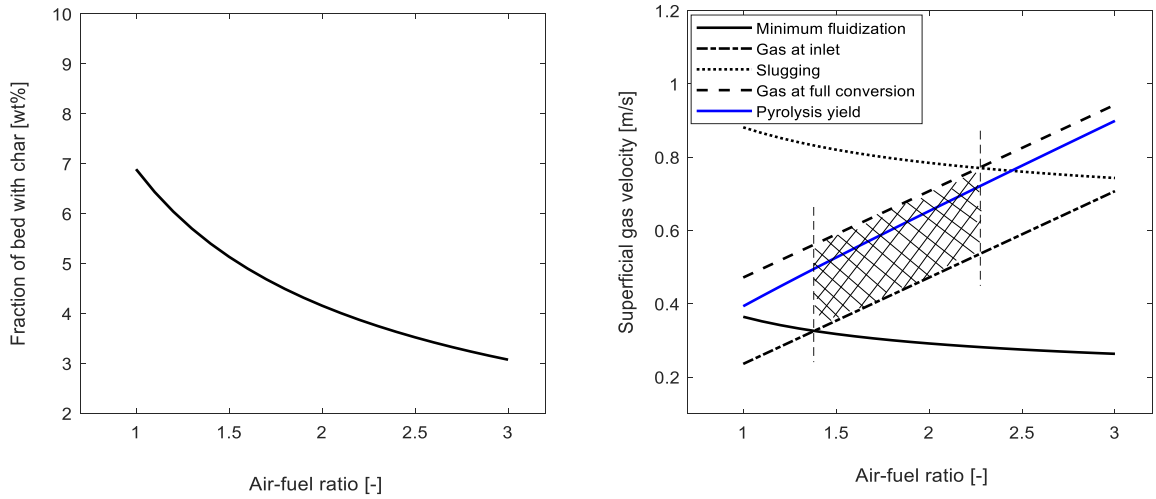

Fig. 4. Behaviour of a bubbling fluidized bed gasifier at constant biomass flowrate, 900 ºC and different air-fuel ratios (a) amount of unconverted char particles (b) gas velocity across the bed showing the safe operating window.

6 Conclusions

This study investigated the behaviour of bubbling fluidized bed in a biomass gasification reactor to illustrate how the operating window can be established. The study applied different correlations proposed in the literature for predicting the minimum fluidization and slugging velocities of a given bed including those of binary mixtures of biomass and bed material. Based on the analysis, the amount of unconverted char particles plays a significant role in the hydrodynamics of the bed, and thus must be considered when selecting the gas velocity for stable operations.

7 References

[1] D. Kunii and O. Levenspiel, Fluidization Engineering, second ed., Butterworth – Heinemann, Washington Street, USA, 1991.

[2] N. Nemati, R. Zarghami, N. Mostoufi, Investigation of hydrodynamics of high temperature fluidized beds by pressure fluctuations, Chem. Eng. Technol. 39 (2016) 1527 – 1536.

[3] R.R. Pattipati, C.Y. Wen, Minimum fluidization velocity at high temperature, Ind. Eng. Chem. Process Des. Dev. 20 (1981) 705 – 708.

[4] J.S.M. Botterill, Y. Teoman, K.R. Yuregir, The effect of operating temperature on the velocity of minimum fluidization, bed voidage and general behaviour, Powder Technol. 31 (1982) 101 – 110.

[5] T. Otake, S. Tone, M. Kawashima, T. Shibata, Behaviour of rising bubbles in a gas fluidized bed at elevated temperature, J. Chem. Eng. Japan 8 (1975) 388 – 392.

[6] Y. Hatate, K. Ijichi, Y. Uemura, M. Migita, D.F. King, Effect of bed temperature on bubble size and bubble rising velocity in a semi-cylindrical slugging fluidized bed, J. Chem. Eng. Japan 23 (1990) 765 – 767.

[7] Si, C.; Guo, Q. Fluidization characteristics of binary mixtures of biomass and quartz sand in an acoustic fluidized bed. Ind. Eng. Chem. Res. 47 (2008) 9773.

[8] Kumoro, A.C.; Nasution, D.A.; Cifriadi, A.; Purbasari, A.; Falaah, A.F. A new correlation for the prediction of minimum fluidization of sand and irregularly shape biomass mixtures in a bubbling fluidized bed. IJAER 9 (2014) 21561.

[9] Ergun, S. Fluid Flow through Packed Column, Chem. Eng. Prog. 48 (1952) 89 – 94.

[10] C.Y. Wen and Y.H. Yu, A Generalized Method for Predicting the Minimum Fluidization Velocity. AIChE J. 12 (1966) 610 – 612.

[11] Agu, C.E., Pfeifer, C., Moldestad, B.M.E, Prediction of void fraction and minimum fluidization velocity of a binary mixture of particles: Bed material and fuel particles, Powder Technol. 349 (2019) 99 – 107.

[12] C.E. Agu, C. Pfeifer, L.-A. Tokheim, B. M.E. Moldestad, Behaviour of Biomass Particles in a Bubbling Fluidized Bed: A Comparison between Wood Pellets and Wood Chips, Chem. Eng. J. 363 (2019) 84 – 98.

[13] J. Baeyens and D. Geldart, An Investigation into Slugging Fluidized Beds, Chem. Eng. Sci. 29 (1974) 255 – 265.

[14] S. Shaul, E. Rabinovich, H. Kalman, Generalized flow regime diagram of fluidized beds based on the height to bed diameter ratio, Powder Technol. 228 (2012) 264 – 271.

[15] C.E. Agu, C. Pfeifer, M. Eikeland, L.-A. Tokheim, B. M.E. Moldestad, Models for predicting average bubble diameter and volumetric bubble flux in deep fluidized beds, Ind. Eng. Chem. Res. 57 (2018) 2658 – 2669.

[16] Agu, C.E., Pfeifer, C., Eikeland, M., Tokheim, L.-A., Moldestad, B.M.E, Measurement and characterization of biomass mean residence time in an air-blown bubbling fluidized bed gasification reactor. Revised and resubmitted to Fuel.

[17] M.J. Andrews, P.J. O'Rourke, The multiphase particle-in-cell (MP-PIC) method for dense particulate flows, Int. J. Multiph. Flow 22 (1996) 379 – 402.

[18] C. Chen, J. Werther, S. Heinrich, H-Y. Qi, E-U. Hartge, CPFD simulation of circulating fluidized bed risers, Powder Technol. 235 (2013) 238 – 247.